HYDROCOASTAL - RACZIW

L2 Processing Algorithms

Specialized SARin retracker: design, development, and utilization on TDS

Sentinel-3 and Cryosat SAR/SARin Radar Altimetry for Coastal Zone and Inland Water

ESA Contract 4000129872/20/I-DT

Project reference: HYDROCOASTAL_ESA_ARESYS_TN_retracking_tool
Issue: 1.0

This page has been intentionally left blank

Change Record

Date	Issue	Section	Page	Comment
10/11/2023	1.0			First Issue

Control Document

Process	Name	Date
Written by:	Aresys	10/11/2023
Checked by		
Approved by:		

Subject	Radar Altimetry for Coastal Zone and Inland Water Level	Project	HYDROCOASTAL - RACZIW
Author	**Organisation**	**Internal references**	
Lisa Recchia	Aresys		
Pietro Guccione	Aresys		
Davide Giudici	Aresys		

	Signature	Date
For HYDROCOASTAL team		
For ESA		

Table of Contents

List of Acronyms

CS2	CryoSat-2
D/D	Delay/Doppler
DEM	Digital Elevation Model
FBR	Full Bit Rate
FFSAR	Fully Focused SAR
UF-SAR	UnFocused SAR
IRF	Impulse Response Function
L1B	Level 1B Product
L1BS	Level a1 Stack Product
OCOG	Offset Centre Of Gravity
POCA	Point Of Closest Approach
PRF	Pulse Repetition Frequency
SAR	Synthetic Aperture Radar
SARin	SAR Interferometric mode
SLC	Single Look Complex
SSH	Sea Surface Height
SWH	Significant Wave Height
S3	Sentinel-3
S6	Sentinel-6
WHS	Water Surface Height

1 Introduction

1.1 The HYDROCOASTAL Project

The HYDROCOASTAL project is a project funded under the ESA EO Science for Society Programme, and aims to maximise the exploitation of SAR and SARin altimeter measurements in the coastal zone and inland waters, by evaluating and implementing new approaches to process SAR and SARin data from CryoSat-2, and SAR altimeter data from Sentinel-3A and Sentinel-3B.

One of the key objectives is to link together and better understand the interactions processes between river discharge and coastal sea level. Key outputs are global coastal zone and river discharge data sets, and assessments of these products in terms of their scientific impact.

1.2 Scope of this Technical Note

The scope of this technical note is the description of the design, development and utilization on TDS of the Specialized SARin retracker.

1.3 Reference Documents

RD-01 RACZIW Technical Proposal, SatOC and RACZIW team, May 2020.

1.4 Document Organisation

After this introductory section, the following sections describe the Specialized SARin retracker: algorithm, the Tool design including Input/output and the main processing steps. A dedicated section is devoted to configuration selection and tool validation results. Finally, the tool delivery dates are reported.

2 Specialized SARin Retracker

Physical retrackers are commonly based on fitting the power waveform with a waveform model. In case of interferometric altimetry, we have three waveforms at Level1:

- Power waveforms
- Coherence waveform
- Phase difference waveforms

The Specialized SARin retracker has been designed on the purpose of fitting jointly the three waveforms.

The main interesting point is to verify if there is an improvement in the quality of the retracked geophysical parameters by exploiting all the information contained in an interferometric acquisition.

Figure below shows the block scheme of the retracker:

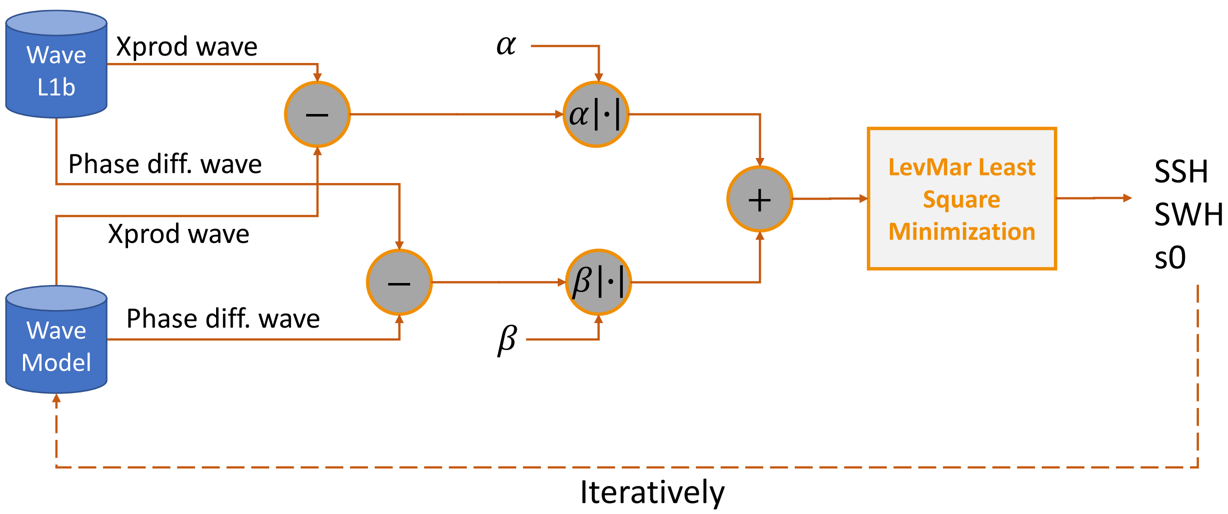

Figure 1. Specialized SARin retracker: algorithm

It can be seen that the core block of the algorithm is the LevMar Least Square Minimization. Here, the objective function to be minimized is the weighted sum of the absolute difference of the two waveforms.

The interfaces of the tool are:

- Inputs:

- CryoSat SARin Level1b product
- Auxiliary files
  - Configuration files (XML and YML)
  - DEM
- Output
- Retracked data file

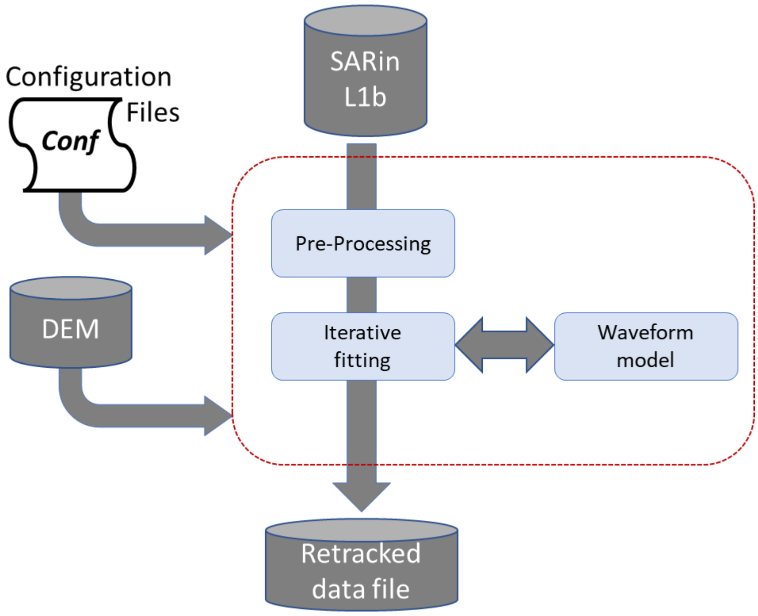

Figure 2. Specialized SARin retracker: interfaces.

The first step is the so called "Pre-processing", which carries out the following tasks:

- extracting from the L1b file the waveforms plus the needed ancillary information
- selecting the subset of waveforms to be processed: SS labelled as ocean are selected
- computing the across-track surface slope from input DEM (optional)

The received radar echo from a uniformly backscattering planar surface can be expressed as function of the delay time t and of look angle ξ by the convolution:

$$W(\tau,\xi) = p_t(\tau) * p_z(\tau) * X(\tau,\xi) \quad \text{Eq. 1.}$$

Where$p_t(\tau)$ is the Instrument range impulse response, $p_z(\tau)$ is the surface height probability density function and $X(\tau,\xi)$ is surface impulse response.

After proper mathematical manipulation, the surface impulse response can be written as:

$$X(\tau,\xi)=\frac{\lambda^2 G_0^2 D_0\ c}{32\pi^2 h^3 \eta} H\left(\tau+\frac{\eta h \xi^2}{c}\right)\int_0^{2\pi} d\vartheta \cdot exp\left[j\frac{2\pi}{\lambda}B(\rho_k sin\vartheta-\chi)\right]\cdot d(\rho_k cos\vartheta-\xi) \cdot exp\left[-2\left(\frac{(\rho_k cos\vartheta-\mu)^2}{\gamma_1^2}+\frac{(\rho_k sin\vartheta-\chi)^2}{\gamma_2^2}\right)\right] \quad \text{Eq. 2.}$$

Where the term $\frac{2\pi}{\lambda}B(\rho_k sin\vartheta-\chi)$ represents the phase difference between two antennas.

2.1 The interferometric waveform model: implementation

Considering the following parameters:

- Instrument parameters
  - PRF
  - Antenna pattern
  - Baseline Length
  - Chirp bandwidth
- Mispointing angles (pitch, roll)
- Surface slope (along and across track slope)
- Height distribution model

Which have been provided to the L1b semi-analytical model, two outputs are obtained:

- *Cross-product waveform: Product of power and coherence waveform*

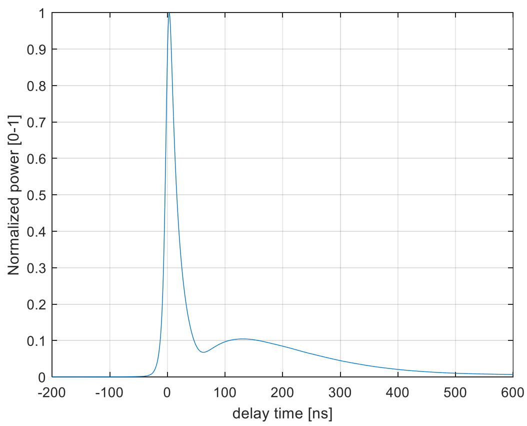

- *Phase difference waveform*

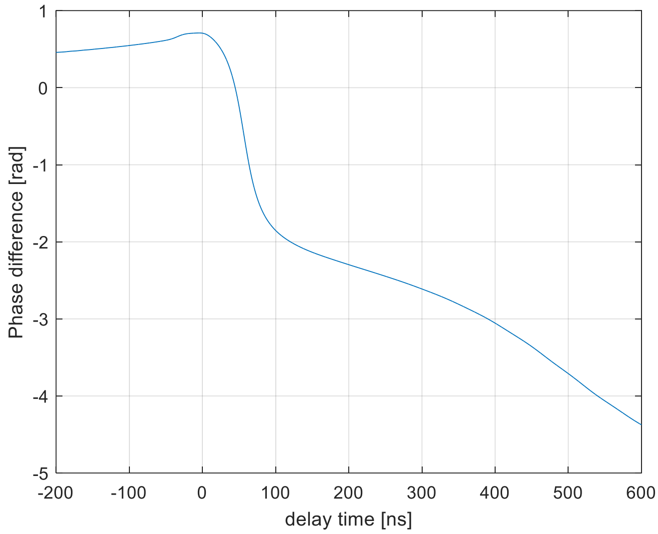

The obtained interferometric waveform model has been validated through a comparison of CryoSat SARin waveforms over ocean and the model waveforms. The visual comparison can be seen in the figures below:

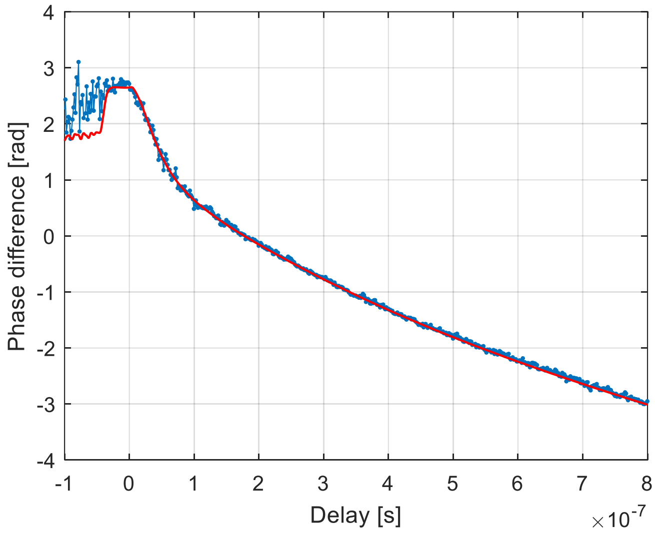

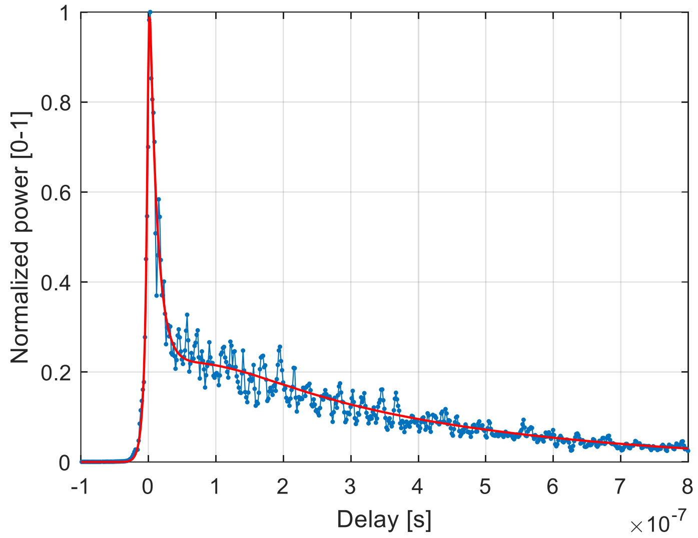

Figure 3. Comparison of CryoSat SARin waveforms over ocean (in blue) and model waveforms (in red).

2.2 Waveform model processing block

This processing block is in charge of computing the theoretical multi-looked SARin waveforms (cross-product and phase difference) that are then used in the iterative fitting procedure.

The block scheme is represented in figure below:

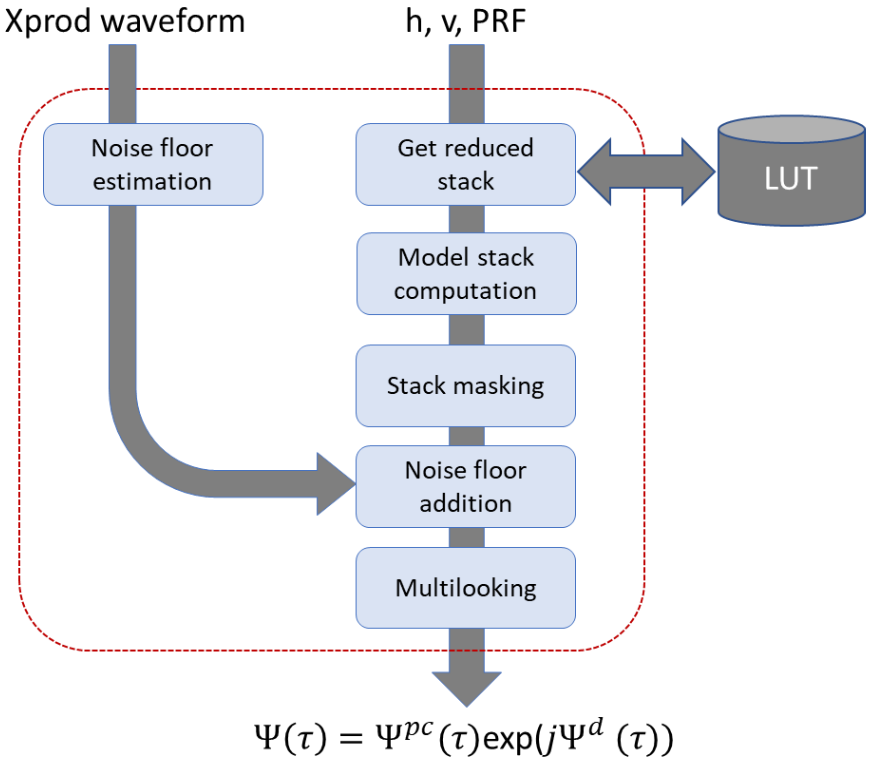

Figure 4. Waveform processing block.

2.3 Iterative fitting

As fitting starting point, the starting values for epoch and SWH are defined. It is possible to limit the fitting of the waveforms in a given interval of samples in the delay direction according to a coherence threshold.

As objective function, the weighted sum of the absolute difference of the two waveforms are computed, as described in the equation below:

$$g(x) = \alpha \cdot \left|\psi^{pc,L1b} - \psi^{pc,mod}(x)\right| + \beta \cdot \left|\psi^{d,L1b} - \psi^{d,mod}(x)\right| \quad \text{Eq. 3.}$$

The actual fitting is performed using iterative Levenberg Marquardt to obtain an estimate of the epoch and of the SWH (Non-linear least square fitting).

The block scheme is represented in figure below:

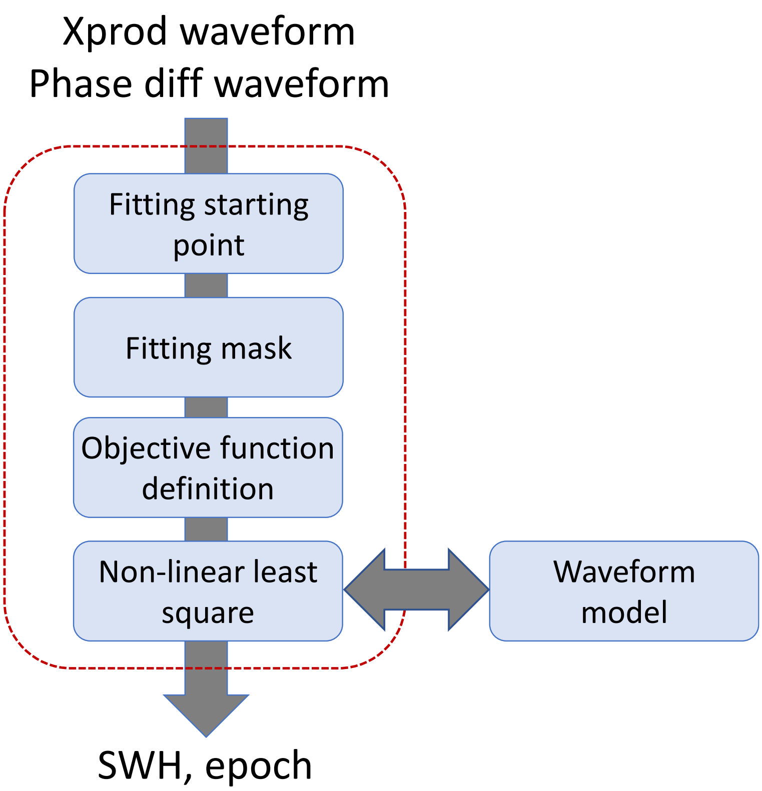

Figure 4. Iterative fitting block scheme.

3 Tool validation and configuration selection

The tool validation has been obtained by comparison of retracked parameters with:

- Aresys power retracker (different implementation based on same theoretical model)
- SAMOSA results

Exploiting the same references, optimal configuration has been selected with respect to:

- Retracking mode
- Retracking objective function
- Coherence thresholds, mask selection, iterative fitting initialization, …

The configuration is reported in the following table:

Processing parameter	Admissible values	Description / Notes
retracking_mode	['P', 'XP']	Retrack waveform from power ('P') or cross product ('XP') stack
objective_function	['of_weighted', 'of_fix_swh']	Name of the objective function used for minimization. Weighted approach ('of_weighted'), phase difference fit with SWH_0 from file ('of_fix_swh'). Power retracking mode 'P' automatically selects 'of_weighted'
cross_product_weight	n/a	Weight assigned to the cross-product waveform in the objective function (used only if retracking_mode == 'XP' and objective_function == 'of_weighted')
phase_difference_weight	n/a	Weight assigned to the phase difference waveform in the objective function (used only if retracking_mode == 'XP' and objective_function == 'of_weighted')
min_coherence	0 – 1	Minimum coherence used to define fitting mask
apply_slope_correction	[0, 1]	Add across-track surface slope to platform roll angle (1=yes, 0=no)
retracking_threshold	0 – 1	Threshold used to coarsely find the leading edge (ratio of max power)

retrack_from_bin_delta	> 0	Bins before leading edge location defining the begin of the fitting mask
retrack_until_bin_delta	> 0	Bins after leading edge location defining the begin of the fitting mask
n_bins_noise_floor	> 0	Number of initial waveform bins used to compute the noise floor

By properly setting the YML configuration file, the following set of processing configuration can be exploited:

Function	**retracking_mode**	**objective_function**	**[cross_product_weight, phase_difference_weight]**	**Notes**
Power	'P'	n/a	n/a	Objective function and weights are assigned automatically
Cross product	'XP'	'of_weighted'	[1, 0]	Retracking of cross product waveform
Phase difference	'XP'	'of_weighted'	[0, 1]	Retracking of phase difference waveform
Phase difference (SSH only)	'XP'	'of_fix_swh'	n/a	Weights are assigned automatically. An input file providing the value of SWH to be used

				needs to be provided

3.1 Tool validation results: comparison with SAMOSA

The figure below shows the comparison of the SSH from the SARIn power retracker (P) and the Aresys power retracker with the SAMOSA retracker. SSH estimates from all retrackers.

It can be noticed that there is a very good agreement and similar noisiness (standard deviation of data averaged along track to 1 Hz).

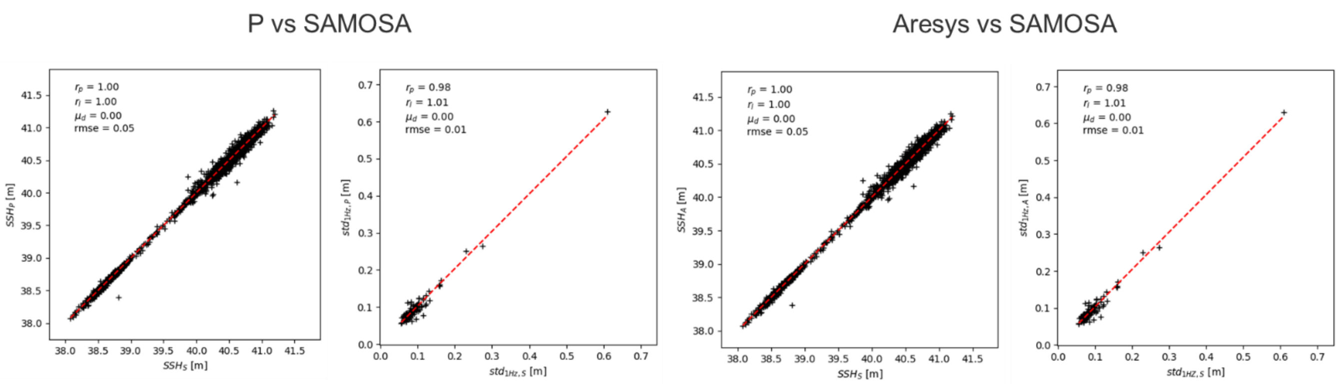

Figure 5. Comparison of the SSH from the SARIn power retracker (P) and the Aresys power retracker with the SAMOSA retracker.

We consider now the validation of the SWH.
The figure below shows the comparison of the SWH from the SARIn power retracker (P) and the Aresys power retracker with the SAMOSA retracker. SWH estimates from all retrackers. Also here, a very good agreement can be noticed, with slightly higher noisiness of SARIn P and Aresys estimates w.r.t. SAMOSA (standard deviation of data averaged along track to 1 Hz)

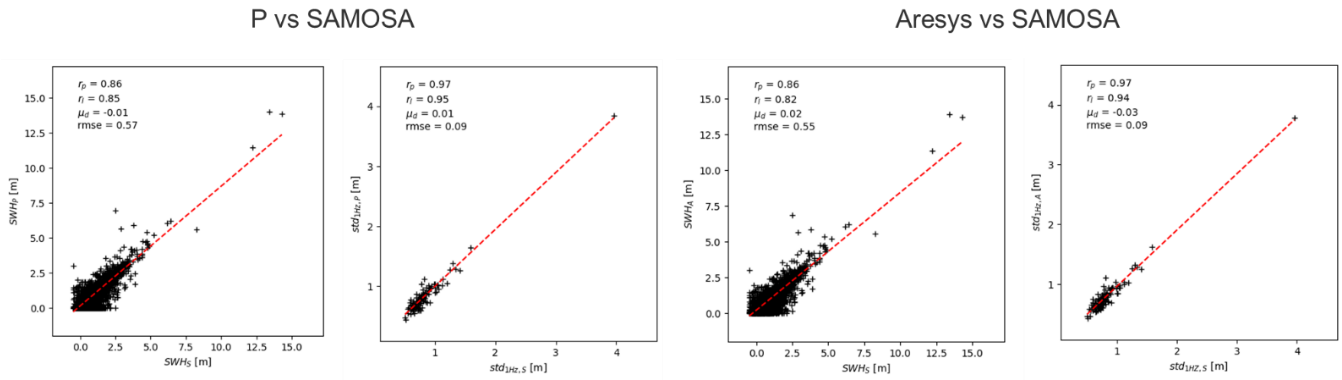

Figure 6. Comparison of the SWH from the SARIn power retracker (P) and the Aresys power retracker with the SAMOSA retracker.

Considering now the phase difference retracker, figure below shows the comparison of the SSH and SWH from the SARIn cross product retracker (XP) with the SAMOSA retracker. SSH and SWH estimates.

It can be noticed a good general agreement but a larger noisiness (standard deviation of data averaged along track to 1 Hz) of XP compared to SAMOSA.

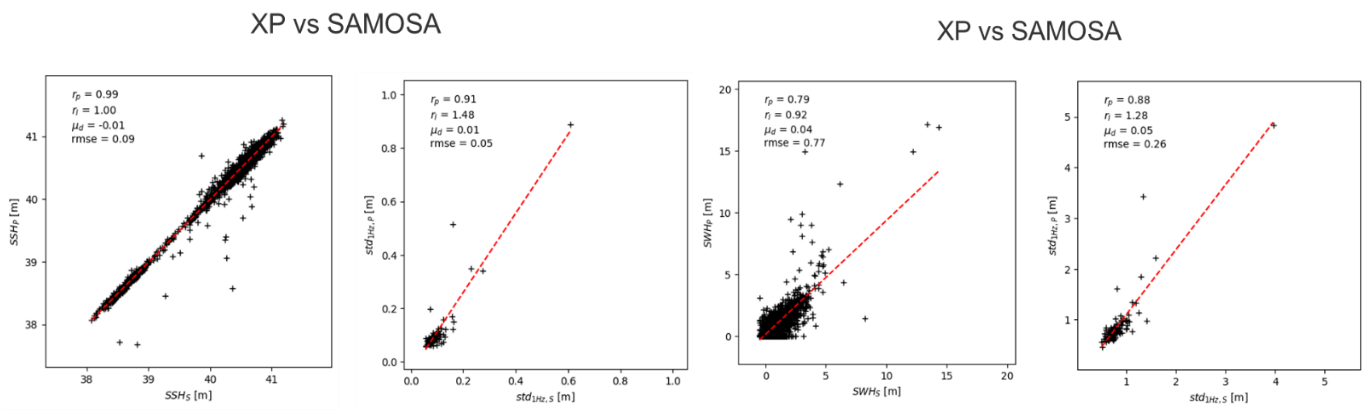

Figure 7. Comparison of the SSH and SWH from the SARIn cross product retracker (XP) with the SAMOSA retracker.

In case SSH from the PD retracker are computed with a given SWH (‘of_fix_swh’ objective function), they show a good correlation with SAMOSA estimates but a larger mean difference. PD SSH is also considerably noisier (standard deviation of data averaged along track to 1 Hz) than SAMOSA estimates. The PD retracker shows no potential for SWH estimation (see figure below).

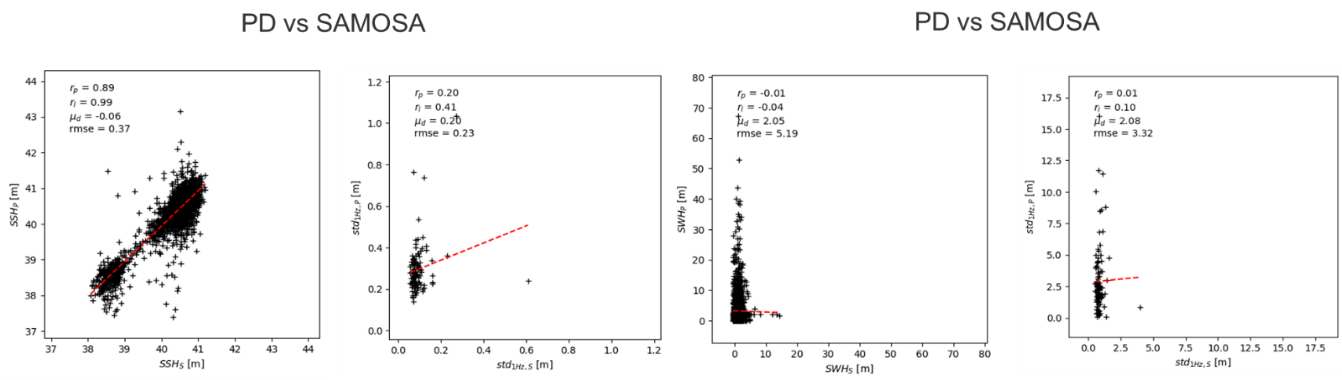

Figure 8. Comparison of the SSH and SWH from the SARIn cross product retracker (XP) with the SAMOSA retracker.

3.2 Tool validation results: analysis on the effect of different minimum coherence thresholds

Comparison of SSH and SWH from the Aresys power retracker with the SARIn power retracker has been considered. Using a minimum coherence of 0.7 (C07) does not seem to improve results compared to no minimum threshold (C00), as reported in the following figure.

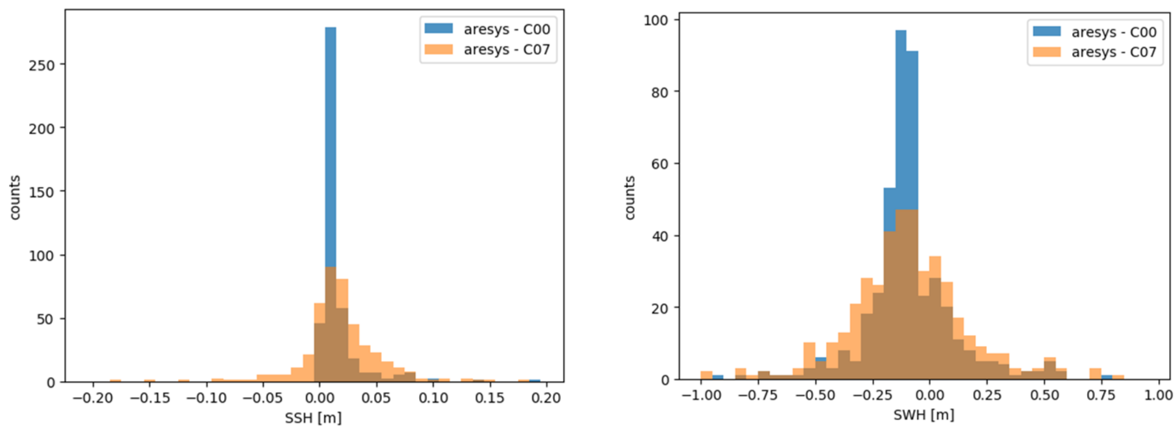

	C00	C07	Aresys	A - C00	A - C07
SSH	-105.64±0.40	-105.65±0.41	-105.63±0.38	0.01±0.02	0.02±0.08
SWH	1.67±1.86	1.67±1.85	1.57±1.74	-0.09±0.20	-0.10±0.47
Misfit	0.17±0.05	0.16±0.05	0.18±0.05	0.01±0.01	0.01±0.02

Figure 9. Analysis on the effect of different minimum coherence thresholds.

In the following, the Comparison of SSH and SWH from the Aresys power retracker with the SARIn cross product retracker is presented.

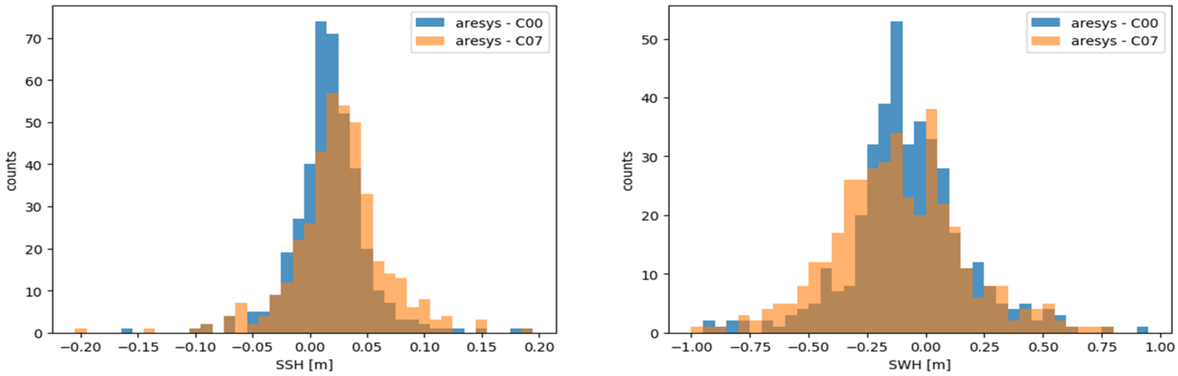

	C00	C07	Aresys	A - C00	A - C07
SSH	-105.73±0.69	-105.74±0.68	-105.63±0.38	0.10±0.35	0.11±0.34
SWH	2.04±2.97	2.09±3.01	1.57±1.74	-0.47±1.55	-0.52±1.64
Misfit	0.21±0.06	0.19±0.07	0.18±0.05	-0.04±0.03	-0.01±0.04

Figure 10. Analysis on the effect of different minimum coherence thresholds.

Basing on the analysis above, the optimal configuration has been selected. It is reported in table below:

Processing parameter	Suggested value	Description / Notes
retracking_mode	‘XP’	Retrack waveform from cross product ('XP') stack
objective_function	‘of_weighted’	Name of the objective function used for minimization. Weighted approach ('of_weighted')
cross_product_weight	1	Weight assigned to the cross-product waveform in the objective function (used only if retracking_mode == 'XP' and objective_function == 'of_weighted')

phase_difference_weight	0	Weight assigned to the phase difference waveform in the objective function (used only if retracking_mode == 'XP' and objective_function == 'of_weighted')
min_coherence	0	Minimum coherence used to define fitting mask
apply_slope_correction	1	Add across-track surface slope to platform roll angle (1=yes, 0=no)
retracking_threshold	0.7	Threshold used to coarsely find the leading edge (ratio of max power)
retrack_from_bin_delta	20	Bins before leading edge location defining the begin of the fitting mask
retrack_until_bin_delta	400	Bins after leading edge location defining the begin of the fitting mask
n_bins_noise_floor	50	Number of initial waveform bins used to compute the noise floor

3.3 Tool validation and configuration selection: main results

From the performed analyses, we can conclude that:

- The power retracker has very similar performance compared to the SAMOSA retracker in terms of both accuracy and noisiness (standard deviation of data averaged along track to 1 Hz).
- The cross-product retracker has an accuracy similar to the power retracker, with a slightly larger noisiness, probably driven by atypical values of coherence in the vicinity of the POCA for some SARIn waveforms over ocean.

- Retracking the phase difference of SARIn waveforms alone does not provide accurate values of SSH/SWH compared with the results from the power retrackers. When providing an optimal value of SWH as an input, the SSH estimates from the phase difference retracker correlate well with those from the power retracker, but with an average difference of ~8 cm, and considerably larger noise

4 Test Dataset

The Cryosat SAR-In data available over Greece have been processed with the specialized SARin retracker tool. This dataset included several SARin acquisitions over sea around Greece coastal zone. In particular, 457 Cryosat-2 SARin L1B Baseline D products have been processed, with dates ranging from June 2028 to May 2020. A summary of the processed dataset is provided in the following table:

TDS	# Files
201806_201808	58
201809_201811	55
201812_201902	56
201903_201905	59
201906_201908	61
201909_201911	55
201912_202002	54
202003_202005	59

5 Tool delivery

The specialized SARin retracker tool version 1.0 was delivered on 24/02/2022.

Delivery package included:

- Altimeter_retracking_v1_0 directory with the tool executables configuration and auxiliary files
- README.txt: a readme text file to guide the user through the installation and test of the tool
- Specialized_SARin_Retracker_Software_User_Manual.pdf: the tool SUM

Version 1.1 of Specialized SARin retracker tool including code optimization has been delivered on 06/04/2022.

6 References

Egido A. and W. H. F. Smith, (2017) "Fully Focused SAR Altimetry: Theory and Applications," in IEEE Transactions on Geoscience and Remote Sensing, vol. 55, no. 1, pp. 392-406, Jan. 2017.

[Ehlers et al., 2022] Ehlers, F., Schlembach, F., Kleinherenbrink, M., and Slobbe, C. (2022). Validity assessment of SAMOSA retracking for fully-focused SAR altimeter waveforms. Advances in Space Research.

Galin N., , D. J. Wingham, R. Cullen, M. Fornari, W. H. F. Smith and S. Abdalla, (2013) "Calibration of the CryoSat-2 Interferometer and Measurement of Across-Track Ocean Slope," in IEEE Transactions on Geoscience and Remote Sensing , vol. 51, no. 1, pp. 57-72, Jan. 2013.

Raney, R. K. , (2014) “Milestones in altimeter performance: Past, present, and future with relevance to coastal altimetry,” presented at the 8th Coastal Altimetry Workshop, Konstanz, Germany, Oct. 23/24, 2014

Ray, C.; Martin-Puig, C.; Clarizia, M.P.; Ruffini, G.; Dinardo, S.; Gommenginger, C.; Benveniste, J., "SAR Altimeter Backscattered Waveform Model," in IEEE Transactions on Geoscience and Remote Sensing, vol.53, no.2, pp.911-919, Feb. 2015.

Scagliola, M., M. Fornari and N. Tagliani, (2015) "Pitch Estimation for CryoSat by Analysis of Stacks of Single-Look Echoes," in IEEE Geoscience and Remote Sensing Letters , vol. 12, no. 7, pp. 1561-1565, July 2015.

Scagliola M., , M. Fornari, J. Bouffard, T. Parrinello, (2018) The CryoSat interferometer: End-to-end calibration and achievable performance, Advances in Space Research, Volume 62, Issue 6, 2018, Pages 1516-1525, ISSN 0273-1177